Electrical conductance map for Saurashtra region, Gujarat, India

P. V. Vijaya Kumar, P. B. V. Subba Rao*, A. K. Singh and C. K. Rao

Indian Institute of Geomagnetism, Panvel, Navi Mumbai 410 218, India

In the present study, we have deployed 35 fluxgate magnetometers and 20 long-period magnetotelluric sites to derive the electrical conductivity distribution of Saurashtra region, Gujarat, India. Geomagnetic field variations (X-north–south, Y-east–west and Z-vertically downward components) recorded at the above sites are investigated to obtain single-station vertical field transfer functions. Maps of induction arrows suggest that the offshore basins are more conducting than inland basins of the region. Thin sheet modelling of the induction features suggests that the anomalous behaviour is strongly influenced by the offshore and shelf edge sedimentary basins that contain thick depo centres of Mesozoic sediments. Jamnagar, Ulva and Mesozoic sedimentary basins on land are also reflected as high conductivity anomalies that could be related to the presence of carbonate/shale sediments. Release of carbon (in the form of thin films) due to thermal activity of Reunion hotspot on carbonate rich sediments may give rise to high conductivity anomalies.

Keywords: Carbon films, induction arrows, thermal activity, thin sheet modelling.

THE Western Continental Margin of India (WCMI) is predominantly affected by the Marion and Reunion hotspot activities[1,2]. Separation of Seychelles plateau from India had taken place ~65 Ma (refs 3, 4) due to Reunion hotspot activity that triggered massive Deccan volcanism in western India. The northwestern part of the Deccan Volcanic Province (DVP) consists of the Saurashtra peninsula (horst-type structure) bounded by Kachchh, Cambay and Narmada rift basins[5].

Geophysical studies carried out in the Saurashtra region, Gujarat, India indicate the presence of underplating mantle material beneath it[6–9]. Seismic tomography studies denote the presence of upper mantle low velocity zone and are attributed to the thermal/chemical anomalies related to the source of Deccan magmatism[10–12]. Mesozoic sediments below the Deccan trap region are delineated using magnetotelluric (MT) methods[13,14]. This technique serves as a guide for delineating the low resistive sediments beneath basalts. Thus, natural electromagnetic methods are used to study the deep structures of sedimentary basins in DVP. Here we develop a regional conductivity model using geomagnetic depth sounding

(GDS) data. Large-scale electrical conductivity structures have been analysed using GDS studies[15–18]. The regional conductance map of Saurashtra was derived by Subba Rao *et al.*[19], showing offshore Surat depression and Saurashtra basins as an anomalous zones using limited sites located in south and central parts of the region. In the present study, we were able to derive the different basins in Saurashtra region due to denser network of stations and thus, enabling us to derive the regional as well as local conductivity anomaly map of Saurashtra and surrounding regions for explaining the observed induction arrows.

In the present study, GDS data (time varying north–south (X), east–west (Y) and vertical (Z) geomagnetic field components) were acquired at 35 sites using Magson fluxgate magnetometers and from 20 long-period magnetotelluric (LMT) stations (Figure 1). Data analysis was carried out by selecting night-time variations to make sure that the inducing field is fairly uniform. The vertical field transfer functions summarizing the relationship between anomalous vertical field component (Z_a) and normal horizontal field components (X_n and Y_n) at a frequency (ω) are described as[15]

$$Z_a(\omega) = T_{zx}(\omega) \times X_n(\omega) + T_{zy}(\omega) \times Y_n(\omega),$$

where all quantities are complex. These transfer functions were computed using robust regression technique for 8–128 min periodicities[20].

Conductivity distribution at the measuring site was extracted from transfer functions through the maps of real and imaginary induction arrows. The magnitude and azimuth of the induction (real/quadrature) arrows are given by

$$S = \mathrm{sqrt}(T_{zx}(\omega)^2 + T_{zy}(\omega)^2)$$

and azimuth of the arrow as

$$\phi = \tan^{-1}(T_{zy}(\omega)/T_{zx}(\omega)).$$

Using Parkinson notation, we have reversed the azimuths so that the arrows point towards the region of current concentration and describe the strike directions of the conductive structures[21]. Figure 2 shows induction arrows for selected periods. Salient features of induction arrows are:

- At short periods, the magnitude of real induction arrows is suppressed over Mesozoic sediments in the central part of the array. Induction arrows in the eastern part point towards Cambay basin and in south they point towards Ulva basin and Surat depression.
- As the period increases from 26 to 85 min, the orientation of induction arrows in the west and central parts of the array changes from NW to WNW direction and
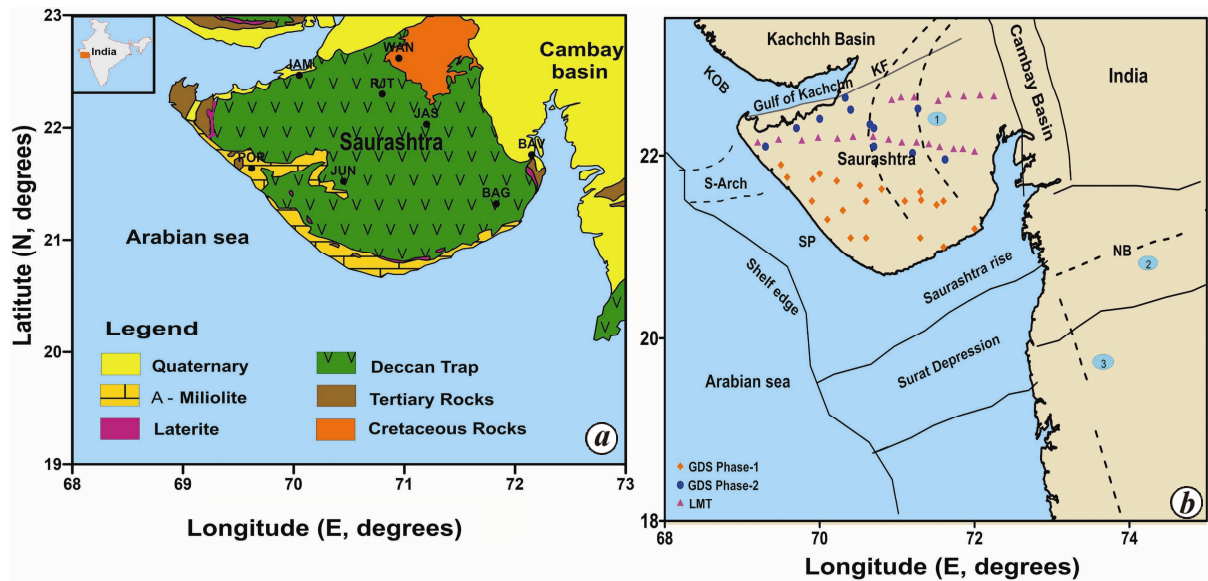
Figure 1. *a*, Geological map of Saurashtra and the surrounding regions (after ref. 38) showing that the entire region is covered by Deccan volcanism. *b*, Various fluxgate magnetometer and long-period magnetotelluric stations installed in different phases. Various tectonic features of the western margin of India (after ref. 39) are also shown. Different Precambrian trends shown are: (1) Delhi–Aravali trend, (2) Satpura trend and (3) Dharwar trend. Offshore Saurashtra arch (S-Arch) is also shown (after ref. 40). KOB, Kachchh offshore basin; SP, Saurashtra Platform; KF, Kaithwari Fault, and NB, Narmada basin. JAM, Jamnagar; WAN, Wanekaner; RJT, Rajkot; JAS, Jasdan; POR, Porbander; JUN, Junagadh; BAV, Bhavnagar; BAG, Bagdana.

points towards offshore region. Induction arrows in the eastern and southern parts rotate from SE to SW direction and point towards the Surat depression.

- The magnitude of induction arrows in the western part of the array is exceeding 1, indicating a large scale regional conductivity anomaly in the offshore Saurashtra basin as observed in the Kachchh array[22]. These regional induced currents follow through a narrow and elongated structure (offshore Saurashtra basin)[23,24] apart from induction due to individual conductive structures.

The purpose of hypothetical event analysis (HEA) is to compute the anomalous vertical field (Z) related to a uniform normal horizontal field of specified polarization[25]. HEA is carried out by estimating Z from the observed transfer functions by taking horizontal magnetic field of unit amplitude and polarization (ϕ). Figure 3 shows HEA carried out for three different periods (8, 26 and 57 min). For 8 min, maximum response is observed at N12°W and it disappears for orthogonal polarization N78°E. Similarly, for 26 min, the response is maximum at N05°W and minimum for N85°E. For these periodicities, anomalous Z/H is observed along the eastern margin of Saurashtra that corresponds to the track of the Reunion hotspot. This anomalous behaviour is absent for 57 min (maximum response is observed for N12°E and disappears for N78°W), and may be attributed to the sediments and mid-crustal anomaly. Presence of low-velocity zone in Cambay basin favours the occurrence of trapped fluids beneath an impermeable layer for the mid-crustal ano-

maly[26,27]. Another interesting feature is that Z/H has a magnitude exceeding 1 in the western part, suggesting channelling of induced currents in the offshore basins of Saurashtra and Kachchh.

Numerical modelling has been carried out for 8 and 26 min periodicities to explain the induction arrows by adopted thin sheet modelling[28]. The sheet was assigned a thickness of 5 km and is considered to be overlying a three-layer model. The choice for the background layered structure is based on long-period magnetotelluric soundings carried out in the Saurashtra region having resistivity values of 1000 and 500 Ωm with a thickness of about 30 and 60 km below which a uniform half space with 50 Ωm, simulates the asthenosphere respectively[29].

In numerical modelling, an area bounded between 68°–74°E and 18°–23°N was chosen and the surface layer representing thin sheet was divided into 120×150 grids with a grid interval 5.5 km. As required by the algorithm, the anomalous domain in the sheet must be enclosed entirely by a uniform region. To minimize the artifact effects due to anomalous domain surrounded by normal structure, the grid was extended to sufficiently large distances away from the observational domain as proposed by Mareschal *et al.*[30].

The numerical computation was carried out to determine (a) the coast effect (due to elecrical conductivity difference between land and sea water) and (b) conductance map that explains the observed induction pattern in Saurashtra region. The calculated coast effect is shown for every site and is significantly small compared to the observed induction arrows at 26 min (Figure 4 *a*). The
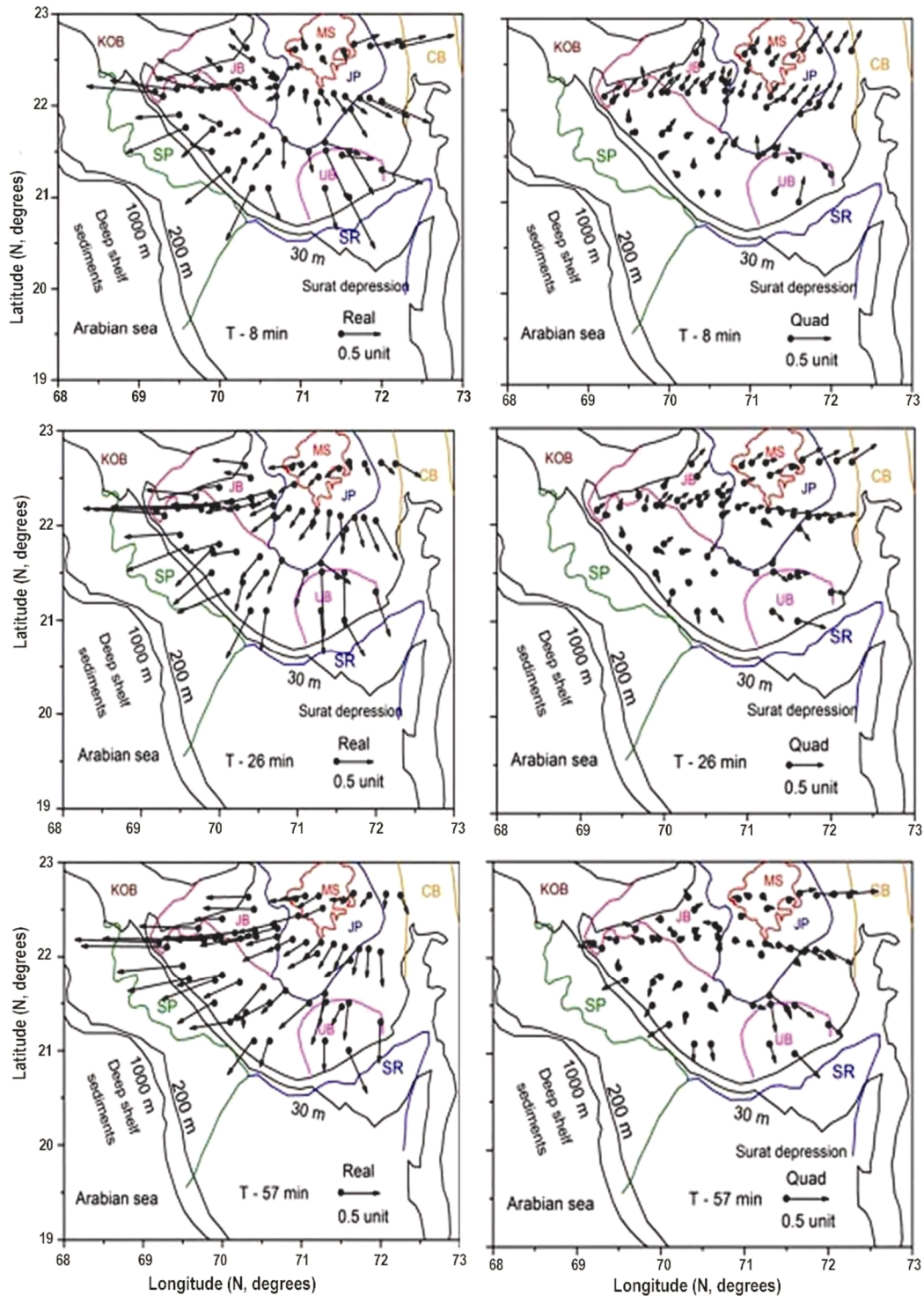
Figure 2. Induction arrows correspond to 8, 26 and 57 min periods. As observed, induction pattern at shorter periods is dominated by the sedimentary basins: Cambay basin (CB), Jamnagar basin (JB), Mesozoic basin (MB; within the Jasdan Plateau (JP)) and Ulve basin (UB). As the period increases, induction arrows in the eastern part rotate from ESE to SW direction and point towards Saurashtra rise (SR) and Surat depression (SD). In the central part over JP, the arrows rotate in the NW direction and point towards JB and KOB, whereas arrows in the south and south-central part point towards UB and SD and in the western part the induction arrows in the WNW direction point towards Saurashtra offshore basin (SOB)/Saurashtra platform (SP). The 200 m bathymetry contour marks the shelf edge.

possible cause could be the wider width of the shelf edge (more than 250 km). According to Biswas[5], several longitudinal extension faults in parallel are responsible for widening of the shelf and differentiating it into several marginal basins. Figure 4 b shows the overall picture of the conductance distribution of Saurashtra region.
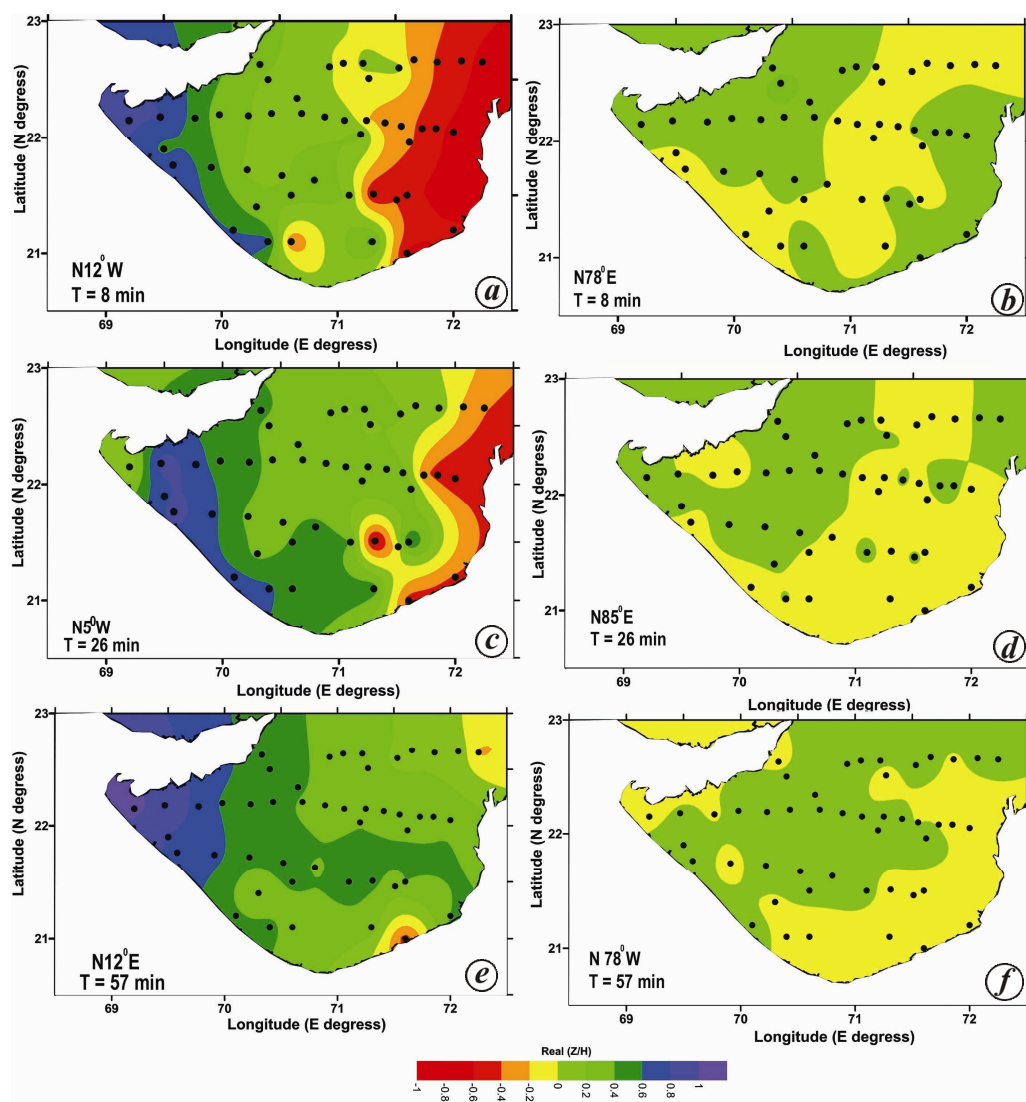
Figure 3. (*a*, *c* and *e*) Contour maps of vertical field *Zr* (after hypothetical event analysis) for all sites for 8, 26 and 57 min periods that bring out the presence of a typical anomaly in the eastern part of the Saurashtra region. This anomalous feature is absent at higher periods. Another interesting feature is high-magnitude *Zr* along the west coast that persists for higher periods. Due to the presence of high resistive body in the west coast, induced currents get deflected through elongated conductive bodies in the form of sediments filling SOB and KOB. The above said anomalies vanish for opposite polarization (*b*, *d* and *f*).

Figure 5 shows a comparison between the observed and model induction arrows, both in its real and quadrature parts.

The observed induction pattern may be explained in terms of an elongated NNW–SSE trending high-conductivity zone (CA-1) in the offshore region related to thick shelf edge sediments containing sandstone and carbonate deposits[31], which continues as an E–W structure in the Gulf of Kachchh. Another major anomaly CA-2 was observed over Surat depression which contains organic-rich shale that has undergone thermal subsidence during Deccan activity and migration of hydrocarbons to Mumbai offshore region[32]. Carbon is generated from carbonate sediments because of thermal activity related to Reunion

hotspot activity. Thus, the presence of carbon and/or black shale within the sedimentary formations may be the source for conductivity anomalies CA-1 and CA-2 (ref. 33).

Different conductivity anomalies CA-3, CA-5, CA-6 and CA-7 were observed over Ulva basin, Jamnagar basin, Mesozoic basin within Jasdan Plateau and Cambay basin with conductivity ranging from 4000 to 8000 S. These anomalies may be attributed to the sediments and precipitation from carbon-rich (CO_2 or CH_4) volatiles associated with underplating event. Additionally, the conductivity anomalies CA-3 and CA-5 were affected by the sea-water transgression and regression. During marine transgression and regression, a vast pile of sedimentation
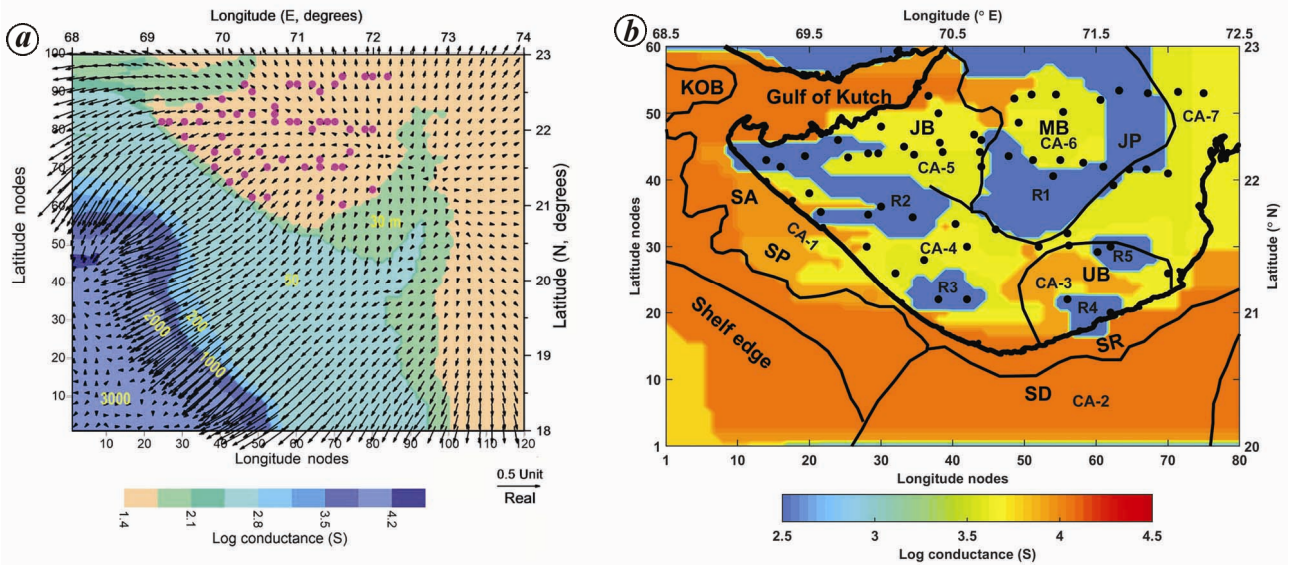
Figure 4. *a*, Calculated coast effect (real induction arrows) at a period of 26 min using 3D thin sheet approximation. It portrays lateral variation in conductance due to land and sea water of variable depth. The arrows are shown for alternate grid points. The calculated coast effect is minimum due to the broader width of the continental shelf. *b*, Thin-sheet conductance map of Saurashtra and the surrounding regions. Different high-conductivity anomalies are observed over the Gulf of Kachchh, KOB, sediments filling shelf edge, SP and SD. In Saurashtra intermediate conductivity anomalies are observed over JB, MB and UB.
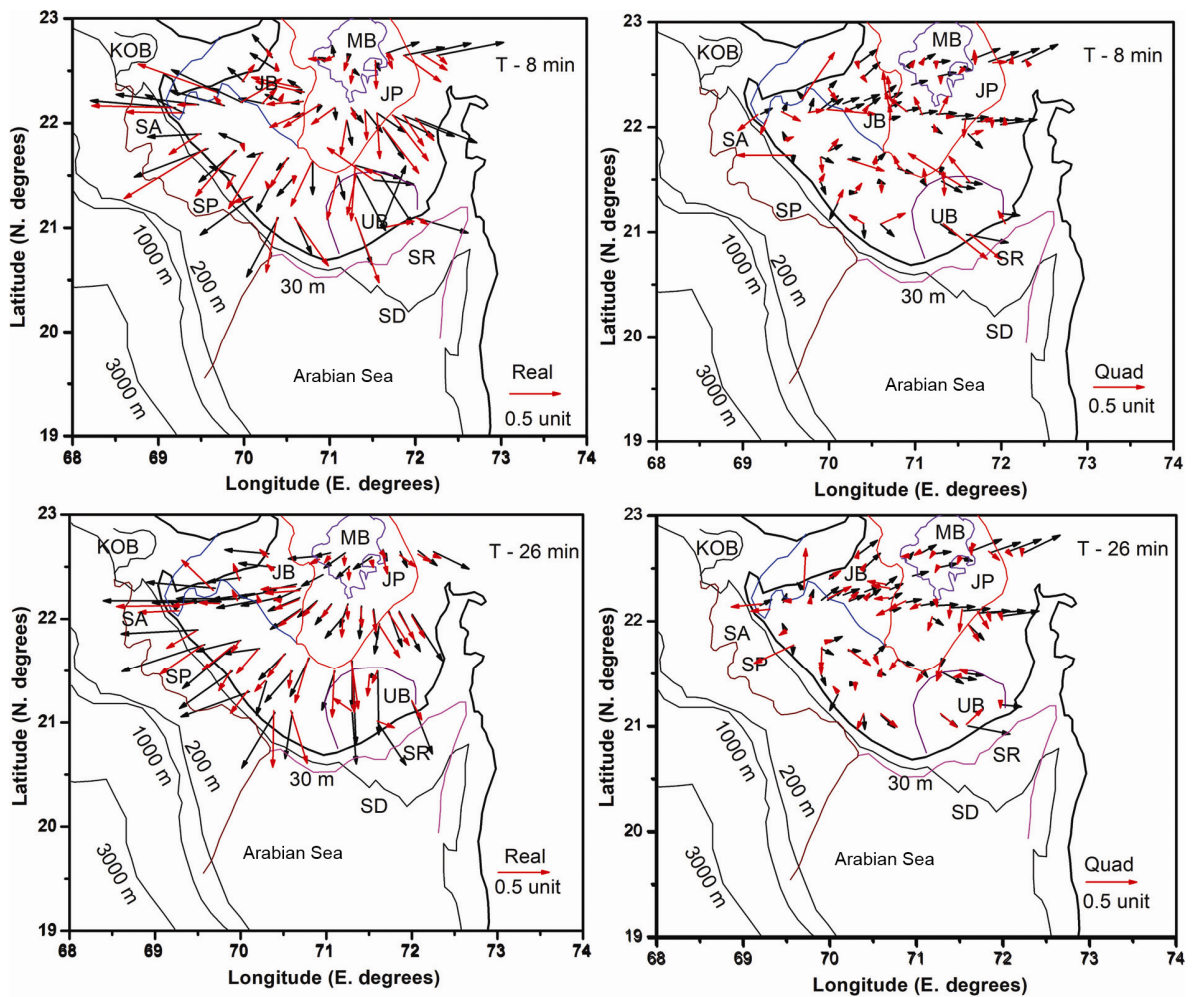

Figure 5. Comparison between the observed (black) and calculated (red) real induction arrows shown for the 8 and 26 min periods.

occurred in the northern part of Jamnagar basin (Gulf of Kachchh) and Ulva basin (Gulf of Khambhat) regions. These saline fluids and sediments have undergone chemical reaction[34]. After chemical reaction these saline fluids invaded into the landward side, causing additional source of conductivity anomalies to CA-3 and CA-5. CA-4 appears to be a transition zone between resistive blocks R1, R2 and R3. Sediments and mid-crustal anomaly in this transition zone may contribute to CA-4.

Different resistivity blocks (R1–R5) may represent volcanic plugs/recrystallization of mafic bodies that may have formed due to the rise of magma through the lithosphere due to the partial melting of the mantle (Reunion hotspot activity). This has been reflected as a shallow Moho beneath R1 in receiver function analysis[9] and shallow basement in resistivity blocks R1–R3 from deep resistivity soundings[35]. Moho depth beneath R2 and R3 (representing Porbander and Junagadh volcanic plugs) was found to increase and appeared to be a deep-seated source-based on geochemical studies[36]. Later, cooling and solidification of magma had given rise to resistive blocks: R1 over a Jasdan plateau, R2 over Porbander, R3 over Jungadh volcanic plugs, and R4 and R5 over Palitana volcanic plugs. R2 extended further north towards Dwaraka/Okha and further offshore region towards Saurashtra arch (S-arch) (Figure 1 *b*). Since currents are deflected by resistive block R2 and channelled through the offshore basins, they will add to the higher magnitude of induction arrows as observed in elongated conductive structures[24]. Similar results were obtained by Arora and Reddy[37] for Valsad region, where induced currents were deflected by resistive volcanic plug or a plutonic body. The resistivity block R2 formed an arch-type structure with a deep basin in between.

Different fluids released during recrystallization of magmatic bodies are an additional source that can contribute to the conductivity anomalies observed over different basins in Saurashtra region. In the present study, conductivity anomalies (CA-1 to CA-7) are related to sedimentary basins, while resistive anomaly is attributed to recrystallized volcanic plugs/plutonic bodies (R1–R5). Offshore regional conductivity anomalies CA-1 and CA-2 are mapped from inland stations. Deploying ocean bottom MT units/ocean bottom magnetometers in the offshore region of Saurashtra and Kachchh will be helpful in deciphering out the electrical conductivity structures in more detail.

1. Storey, M., Mahoney, J. J., Saunders, A. D., Duncan, R. A., Kelley, S. P. and Coffin, M. F., Timing of hot spot related volcanism and the breakup of Madagascar from India. *Science*, 1995, **267**, 852–855.
2. Morgan, W. J., Plate motions and deep mantle convection. *Mem. Geol. Soc. Am.*, 1972, **132**, 7–22.
3. White, R. S. and McKenzie, D., Magmatism at rift zones: the generation of volcanic continental margins and flood basalts. *J. Geophys. Res.*, 1989, **94**, 7685–7729.
4. White, R. S. and McKenzie, D., Mantle plumes and flood basalts. *J. Geophys. Res.*, 1995, **100**, 17543–17585.
5. Biswas, S. K., Regional tectonic framework, structure and evolution of the western marginal basins of India. *Tectonophysics*, 1987, **135**, 307–327.
6. Radhakrishana, M., Verma, R. K. and Purushotham, A. K., Lithospheric structure below the eastern Arabian Sea and adjoining west coast of India based on intergrated analysis of gravity and seismic data. *Mar. Geophys. Res.*, 2002, **23**, 25–42.
7. Rao, G. S. P. and Tewari, H. C., The seismic structure of the Saurashtra crust in NW India and its relationship to Reunion hotspot. *Geophys. J. Int.*, 2005, **160**, 318–330.
8. Tewari, H. C., Surya Prakasa Rao, G. and Rajendra Prasad, B., Uplifted crust in parts of western India. *J. Geol. Soc. India*, 2009, **73**, 479–488.
9. Chopra, S. *et al.*, Crustal structure of the Gujarat region, India: new constraints from the analysis of teleseismic receiver functions. *J. Asian Earth Sci.*, 2014, **96**, 237–254.
10. Kennett, B. L. N. and Widiyantoro, S., A low seismic wave speed anomaly beneath North Western India: a seismic structure of Deccan hotspot? *Earth Planet. Sci. Lett.*, 1999, **165**, 145–155.
11. Mohan, G., Ravi Kumar, M., Saikia, D., Praveen Kumar, K. A., Tiwari, P. Kr. and Surve, G., Imprints of volcanism in the upper mantle beneath NW Deccan volcanic Province. *Lithosphere*, 2012, **4**, 150–159.
12. Madhusudhan Rao, K., Ravi Kumar, M., Rastogi, B. K., Crust beneath the northwestern Deccan Volcanic Province, India: evidence for uplift and magmatic underplating. *J. Geophys. Res.*, 2015, **120**, 3385–3405.
13. Sarma, S. V. S., Patro, B. P. K., Harinarayana, T., Veeraswamy, K., Sastry, R. S. and Sarma, M. V. C., A magnetotelluric (MT) study across the Koyna seismic zone, western India: evidence for block structure. *Phys. Earth Planet. Inter.*, 2004, **142**, 23–36.
14. Patro, P. K. *et al.*, Sub-basalt sediment imaging – the efficacy of magnetotellurics. *J. Appl. Geophys.*, 2015, **121**, 106–115.
15. Schmucker, U., Anomalies of geomagnetic variations in the southwestern United States. *Bull. Scripps Inst. Oceanogr.*, 1970, **13**, 1–165.
16. Beamish, D., The mapping of induced currents around the Kenyarift: comparison techniques. *Geophys. J. R. Astron. Soc.*, 1977, **50**, 311–322.
17. Arora, B. R., Rigoti, A., Vitorello, I., Padhila, A. L., Trivedi, N. B. and Chamalaun, F. H., Electrical imaging of the intracratonic Parnaiba basin, North–Northeast Brazil. *J. Geomagn. Geoelectr.*, 1997, **49**, 1631–1648.
18. Arora, B. R. and Subba Rao, P. B. V., Integrated modeling of EM response functions from peninsular India and Bay of Bengal. *Earth Planets Space*, 2002, **54**, 637–654.
19. Subba Rao, P. B. V., Singh, A. K. and Rao, C. K., Regional conductance map of Saurashtra and surrounding regions. *Curr. Sci.*, 2012, **103**(2), 187.
20. Egbert, G. D. and Booker, J. R., Imaging crustal structure in southwestern Washington with small magnetometer arrays. *J. Geophys. Res.*, 1993, **98**, 15967–15985.
21. Lilley, F. E. M. and Arora, B. R., The sign convention for quadrature Parkinson arrows in geomagnetic induction studies. *Rev. Geophys.*, 1982, **20**, 513–518.
22. Subba Rao, P. B. V., Arora, B. R. and Singh, A. K., Electrical conductance map for the Kachchh rift basin: constraint on tectonic evolution and seismotetonic implications. *Pure Appl. Geophys.*, 2014, **171**, 2353–2370.
23. Jones, A. G., The problem of current channeling: critical review. *Geophys. Surv.*, 1983, **6**, 79–122.
24. Arora, B. R. and Adam, A., Anomalous directional behaviour of induction arrows above elongated conductive structures and its possible causes. *Phys. Earth Planet. Inter.*, 1992, **74**, 183–190.

25. Bailey, R. C., Edwards, G. D., Garland, G. D., Kurtz, R. and Pitcher, D., Electrical conductivity studies over a tectonically active area in eastern Canada. *J. Geomagn. Geoelectr.*, 1974, **26**, 125–146.

26. Kaila, K. L., Tewari, H. C., Krishna, V. G., Dixit, M. M., Sarkar, D. and Reddy, M. S., Deep seismic sounding studies in the north Cambay and Sanchor basin, India. *Geophys. J. Int.*, 1990, **103**, 621–637.

27. Dixit, M. M., Tewari, H. C. and Visweswara Rao, C., Two-dimensional velocity model of the crust beneath the South Cambay Basin, India from refraction and wideangle reflection data. *Geophys. J. Int.*, 2010, **181**, 635–652.

28. Vasseur, G. and Weidelt, P., Bimodel electromagnetic induction in non-uniform thin sheets with an application to the northern Pyrenean induction anomaly. *Geophys. J. R. Astron. Soc.*, 1977, **51**, 669–690.

29. Vijaya Kumar, P. V., Subba Rao, P. B. V., Rao, C. K., Singh, A. K. and Rama Rao, P., Frequency characteristics of geomagnetic induction anomaliesin Saurashtra Region. *J. Earth Sci. Syst.* 2017, 101; doi:10.1007/s12040-017-0872-5.

30. Mareschal, M., Vasseur, G., Srivastava, B. J. and Singh, R. N., Induction models of southern India and effect of offshore geology. *Phys. Earth Planet. Inter.*, 1987, **45**, 137–148.

31. Sharma, K., Nilesh, B., Shukla, A. D., Cheong, D. K. and Singhvi, A. K., Optical dating of late Quaternary carbonate sequence of Saurashtra, western India. *Quaternary Res.*, 2017, **87**, 133–150.

32. Dwivedi, A. K., Petroleum exploration in India – a perspective and endeavours. *Proc. Indian Natl. Sci. Acad.*, 2016, **82**, 881–903.

33. Duba, A., Huenges, E., Nover, G. and Will, G., Impedance of black shale from the Munster land I borehole: an anomalously good conductor. *Geophys. J. Int.*, 1988, **94**, 413–419.

34. Chamyal, L. S., Maurya, D. M. and Rachna Raj, Fluvial systems of the drylands of western India: a synthesis of Late Quaternary environmental and tectonic changes. *Quaternary Int.*, 2003, **104**, 69–86.

35. Singh, S. B. *et al.*, Delineation of basaltic covered sediments in the Saurashtra region using deep resistivity sounding studies. In Fifth Conference and Exposition on Petroleum Geophysics, Hyderabad, 2004, 69–74.

36. Chandrasekhar, D. V., Mishra, D. C., Rao, G. P. and Rao, J. M., Gravity and magnetic signatures of volcanic plugs related to Deccan volcanism in Saurashtra, India and their physical and geochemical properties. *Earth Planet. Sci. Lett.*, 2002, **201**, 277–292.

37. Arora, B. R. and Reddy, C. D., Magnetovariational study over a seismically active area in the Deccan trap province of western India. *Phys. Earth Planet. Int.*, 1991, **66**, 118–131.

38. Merh, S. S., *Geology of Gujarat*, Geological Society of India Publication, Bangalore, 1995, pp. 1–222.

39. Biswas, S. K., A review of structure and tectonics of Kutch basin, western India, with special reference to earthquakes. *Curr. Sci.*, 2005, **88**, 1592–1600.

40. Bhattacharya, G. C. and Subramanyam, V., Extension of the Narmada–Son lineament on the continental margin off Saurashtra, western India as obtained from magnetic measurements. *Marine Geophys. Res.*, 1986, **8**, 329–344.

Response of fish communities to abiotic factors in Western Ramganga, Kumaun Lesser Himalaya, India

Shahnawaz Ali*, N. N. Pandey, Prem Kumar, Ravindar Posti and A. K. Singh

ICAR-Directorate of Coldwater Fisheries Research, Bhimtal 263 136, India

Abiotic factors in the riverine ecosystem are important in structuring fish communities along the longitudinal gradients. Quantitative data on species abundance were collected during October 2015–September 2016 in the mountain stretch of the River Western Ramganga from Kumaun Lesser Himalayas, India. Multivariate analyses were done to study the relationship between fish assemblages and abiotic parameters. Cluster analysis and non-metric multidimensional scaling indicated two distinct groups in the upstream and downstream zones. The composition of fish assemblages in different zones was found to be strongly associated with habitat characteristics. Canonical correspondence analysis revealed species abundance association with temperature, conductivity, stream width and altitude. Further analysis showed conductivity–altitude combination as the primary factor determining the longitudinal distribution of species composition in the studied stretch of this river. The present study aids in understanding the factors that determine the spatial segregation of species for the restoration, conservation and management of aquatic resources.

Keywords: Abiotic factors, assemblage structure, fish communities, multivariate analysis, riverine ecosystem.

THE riverine or lotic ecosystem consists of rich and varied biota, including diverse fish species adapted to the different environmental factors operating in the habitat[1]. The fish community structure varies along the upstream–downstream gradient of river ecosystems on a spatial and temporal scale as a result of differences in habitat structure and resource availability[1,2]. Moreover, changes in different biotic (e.g. competition, predation) and abiotic factors such as channel morphology, stream order, water quality, stream flow regimes and temperature operating at local and regional scale also influence the species richness and diversity within a river basin[1–5]. Fish communities in a riverine system are also sensitive to changes in multiple environmental factors. Accordingly, they have widely been employed for studying the ecological integrity and well-being of biological communities in the freshwater ecosystem[6–8]. Apart from natural regulation of species distribution, human alterations to stream